B hadron production and decay at ATLAS

E Bouhova-Thacker, on behalf of the ATLAS Collaboration

Physics Department, Lancaster University, Lancaster LA1 4YB, UK

E-mail: e.bouhova-thacker@lancaster.ac.uk

Abstract. Selected recent B-physics results published by the ATLAS experiment at the LHC are presented. The Λ_b^0 parity-violating decay asymmetry parameter, α_b, is measured to be $0.30 \pm 0.16(\text{stat}) \pm 0.06(\text{syst})$. A new excited state of the $B_c^\pm$ meson is observed with a mass $6842 \pm 4(\text{stat}) \pm 5(\text{syst})$ MeV, consistent with expectations for the second S-wave state of the $B_c^\pm$ meson, $B_c^\pm(2S)$.

1. Introduction

Results by the ATLAS Collaboration on the measurement of the parity-violating asymmetry parameter α_b and the helicity amplitudes for the decay $\Lambda_b^0 \to J/\psi \Lambda^0$ [1] and on the observation of an excited $B_c^\pm$ meson state [2] are reported.

2. Parity violation and helicity amplitudes in $\Lambda_b^0 \to J/\psi(\mu^+\mu^-)\Lambda^0$ decays

Parity violation in hadron weak decays is not maximal and depends on the hadron's constituents. For heavy baryons, theoretical predictions are possible using perturbative QCD and the Factorisation Approximation [3] or Heavy Quark Effective Theory (HQET) [4]. The decay asymmetry parameter, α, of a two-body spin-$\frac{1}{2}$ particle decay can be extracted from the angular distribution $\frac{dN}{d\cos\theta} = \frac{1}{2}(1 + P\alpha\cos\theta)$, where θ is the angle between the polarisation vector and the direction of the decay product in the particle's rest frame. Due to the symmetries of the initial state and the ATLAS detector [5], $P(p_T, \eta) = -P(p_T, -\eta)$, the average polarisation is zero, and a full angular analysis is required to extract α. The $\Lambda_b^0 \to J/\psi \Lambda^0$ decay can be described by four helicity amplitudes $A(\lambda_{\Lambda^0}, \lambda_{J/\psi})$: $a_+ = |a_+|e^{i\rho_+} \equiv A(1/2, 0)$, $a_- = |a_-|e^{i\rho_-} \equiv A(-1/2, 0)$, $b_+ = |b_+|e^{i\omega_+} \equiv A(-1/2, -1)$, $b_- = |b_-|e^{i\omega_-} \equiv A(1/2, 1)$, where λ_{Λ^0} and $\lambda_{J/\psi}$ are the helicities of Λ^0 and J/ψ. The full angular probability density function (PDF) of the decay angles $\Omega = (\theta, \theta_1, \phi_1, \theta_2, \phi_2)$, where θ_1 (θ_2) and ϕ_1 (ϕ_2) are the polar and azimuthal angles of the proton (μ^+) in the Λ^0 (J/ψ) rest frame with respect to the Λ^0 (J/ψ) direction in the Λ_b^0 rest frame, is given as

$$w(\Omega, A, P) = \frac{1}{(4\pi)^3} \sum_{i=0}^{19} f_{1i}(A) f_{2i}(P, \alpha_{\Lambda^0}) F_i(\Omega).$$

The F_i are orthogonal functions of the decay angles, multiplied by functions of the helicity amplitudes and the polarisation. As $\langle P \rangle = 0$ only six terms are non-zero. The five independent parameters are chosen as: $\alpha_b = |a_+|^2 - |a_-|^2 + |b_+|^2 - |b_-|^2$, $k_+ = \frac{|a_+|}{\sqrt{|a_+|^2 + |b_+|^2}}$, $k_- = \frac{|a_-|}{\sqrt{|a_-|^2 + |b_-|^2}}$, $\Delta_+ = \rho_+ - \omega_+$ and $\Delta_- = \rho_- - \omega_-$. The analysis extracts α_b and the helicity amplitudes from the measured averages $\langle F_i \rangle = \frac{1}{N^{data}} \sum_{n=1}^{N^{data}} F_i(\Omega_n)$ with a least squares fit.

The analysis uses $4.6\,\mathrm{fb}^{-1}$ of 7 TeV data collected with single-muon and $J/\psi \to \mu\mu$ triggers. A mass constrained cascade fit is performed with a J/ψ and Λ^0 mass constraints to the world average values [6] and requiring that the Λ^0 momentum points to the di-muon vertex. Cuts are applied on the fit quality, $\chi^2/N_{dof} < 3$, the transverse momentum of Λ^0, $p_T^{\Lambda^0} > 3.5$ GeV, the transverse decay length of Λ^0, measured from the Λ_b^0 vertex, $L_{xy}^{\Lambda^0} > 10$ mm, and the Λ_b^0 proper decay time, $\tau > 0.35$ ps. A B_d hypothesis is also considered and candidates are kept if the Λ_b^0 hypothesis has the larger cumulative χ^2 probability, $\mathcal{P}_{\Lambda_b^0} > \mathcal{P}_{B_d}$. Figure 1 shows the invariant mass of the reconstructed Λ_b^0 and $\bar{\Lambda}_b^0$ candidates. CP invariance is assumed.
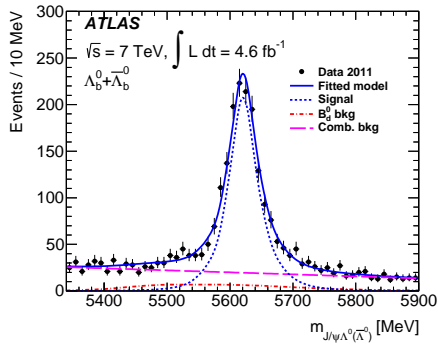

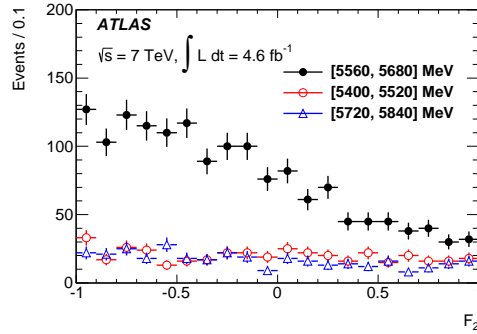**Figure 1.** The reconstructed mass of Λ_b^0 and $\bar{\Lambda}_b^0$ candidates.

Figure 2. F_2 distribution for the signal and sideband regions.

An extended binned maximum likelihood fit is performed to extract the signal. Monte Carlo templates are used to describe the Λ_b^0 and B_d mass shapes and the combinatorial background is parametrised by a first-order polynomial. The distribution of F_2 in the signal and background regions is shown in figure 2. The two sideband distributions are similar and the average is used to subtract from the signal. The parameters are extracted by minimising $\chi^2 = \sum_i \sum_j (\langle F_i \rangle^{exp} - \langle F_i \rangle) V_{ij}^{-1} (\langle F_j \rangle^{exp} - \langle F_j \rangle)$, where V is the covariance matrix of the moments, $\langle F_i \rangle$. The expected values are given by $\langle F_i \rangle^{exp} = \sum_j f_{1j}(A) f_{2j}(\alpha_{\Lambda^0}) C_{ij}$, where $C_{ij} = \frac{1}{(4\pi)^3} \iint F_i(\Omega') T(\Omega', \Omega) F_j(\Omega) d\Omega' d\Omega \approx \frac{\epsilon_T}{N^{MC}} \sum_{n=1}^{N^{MC}} F_i(\Omega'_n) F_j(\Omega_n)$. $T(\Omega', \Omega)$ accounts for acceptance and detector effects, while ϵ_T is determined using the identity $\langle F_0 \rangle^{exp} = 1$.
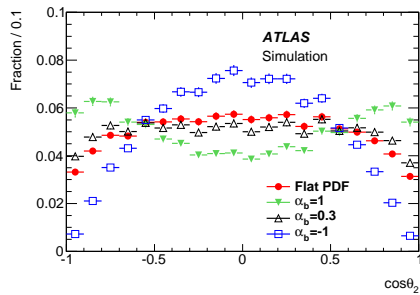

Figure 3. $\cos \theta_2$ distribution, after detector effects, for different values of α_b, $k_+ = 0.21$, $k_1 = 0.134$, $\Delta_\pm = 0$.
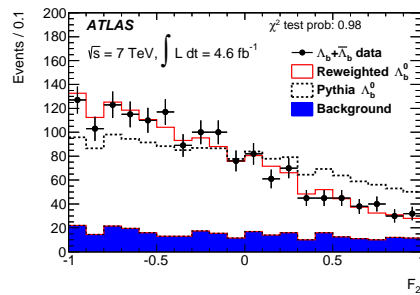

Figure 4. F_2 distribution from the sum of the weighted MC events and the background, compared to data.

Figure 3 shows one of the angular distributions after acceptance, efficiency and resolution effects are taken into account. To illustrate the ATLAS sensitivity the events are weighted with

different values for α_b. The Monte Carlo (MC) events are generated with uniform distributions. After extracting the parameters, the MC signal distributions are re-weighted using the measured parameters, added to the background distributions and compared to data. Figure 4 shows good agreement between data and re-weighted MC. The main sources of systematic uncertainty are from the background shape modelling and the limited MC statistics.

The measured values of $\langle F_i \rangle$, after sideband subtraction and B_d correction, yield the following values for the parameters and helicity amplitudes:

$$\alpha_b = 0.30 \pm 0.16(\text{stat}) \pm 0.06(\text{syst}) \qquad |a_+| = 0.17^{+0.12}_{-0.17}(\text{stat}) \pm 0.09(\text{syst})$$

$$k_+ = 0.21^{+0.14}_{-0.21}(\text{stat}) \pm 0.13(\text{syst}) \qquad |a_-| = 0.59^{+0.06}_{-0.07}(\text{stat}) \pm 0.03(\text{syst})$$

$$k_- = 0.13^{+0.20}_{-0.13}(\text{stat}) \pm 0.15(\text{syst}) \qquad |b_+| = 0.79^{+0.04}_{-0.05}(\text{stat}) \pm 0.02(\text{syst})$$

$$|b_-| = 0.08^{+0.13}_{-0.08}(\text{stat}) \pm 0.06(\text{syst}).$$

The value of α_b is consistent with a recent LHCb measurement, $\alpha_b = 0.05 \pm 0.17(\text{stat}) \pm 0.07(\text{syst})$ [7], and lies between the pQCD [3], (α_b in the range -0.17 to -0.14) and HQET [4] ($\alpha_b = 0.78$) predictions. The large values of $|a_-|$ and $|b_+|$ suggest a negative helicity for Λ^0.

3. Observation of an excited $B_c^\pm$ meson state

The spectrum and properties of the B_c family are predicted by non-relativistic potential models, perturbative QCD and lattice calculations [8]. The second S-wave state is expected to have a mass in the range $m_{B_c(2S)} \sim 6835\text{—}6917$ MeV. The pseudo-scalar and vector spin states cannot be separated by this analysis. The ATLAS experiment observe a peak structure in the mass difference distribution

$$Q = m(B_c^\pm \pi\pi) - m(B_c^\pm) - 2m(\pi^\pm).$$

The ground state is observed in the $B_c^\pm \to J/\psi(\mu^+\mu^-)\pi^\pm$ decay mode.

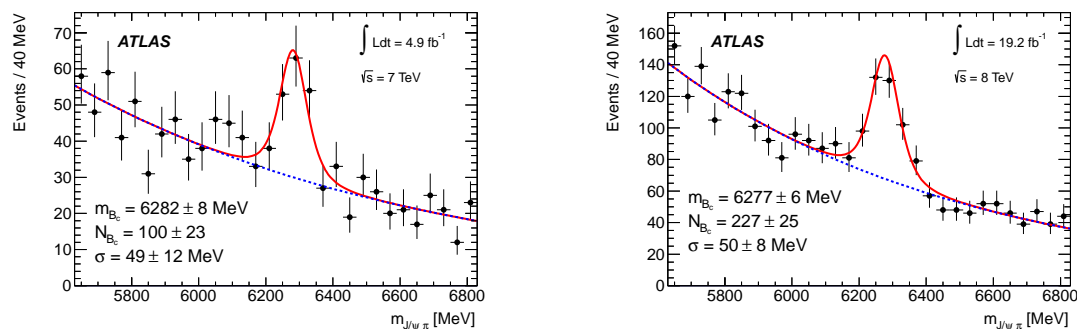**Figure 5.** Invariant mass distribution of the reconstructed $B_c^\pm \to J/\psi(\mu^+\mu^-)\pi^\pm$ candidates in 7 (left) and 8 (right) TeV data.

The analysis uses $4.9\,\text{fb}^{-1}$ of 7 TeV and $19.2\,\text{fb}^{-1}$ of 8 TeV data collected with $J/\psi \to \mu\mu$ triggers. The analysis is optimised separately for the two centre-of-mass energies due to different pile-up conditions. $B_c^\pm$ candidates are reconstructed using a mass constrained fit. The combinatorial background is reduced using an impact parameter cut, $d_0^{\pi^\pm}/\sigma(d_0^{\pi^\pm}) > 5\,(4.5)$ for the 7 (8) TeV data. The fitted $B_c^\pm$ mass, shown in figure 5, is consistent with the world average [6]. Both distributions are fitted separately using an extended unbinned maximum likelihood fit, with a Gaussian (exponential) function modelling the signal (background) shape. The stability of the $B_c^\pm$ yield is checked through its normalisation to $B^\pm \to J/\psi(\mu^+\mu^-)K^\pm$ decays, reconstructed with similar requirements.

$B_c^\pm$ candidates in $\pm 3\sigma$ mass window of the fitted mass value of each dataset are combined with two tracks from the corresponding primary vertex in a cascade fit with a J/ψ mass constraint and requiring that the $B_c^\pm$ momentum points to the $B_c^\pm(2S)$ vertex. An unbinned maximum likelihood fit gives the following values for the mass of the observed structure: 288.2 ± 5.1 MeV and 288.4 ± 4.8 MeV for the 7 and 8 TeV datasets. The corresponding values for the widths of the structure are 18.2 ± 3.8 MeV and 17.6 ± 4.0 MeV. All uncertainties are statistical only. The Q distributions for the 7 and 8 TeV data are shown in figure 6.

The fit includes a third-order polynomial to model the background and a Gaussian function for the structure. The relative $B_c^\pm(2S)/B_c^\pm$ yield ratio is verified to be statistically consistent between the 7 TeV and 8 TeV data. The main contributions to the systematic uncertainty come from the pion momentum scale, the uncertainty on the mass of the ground state and the signal and background models. The total averaged systematic uncertainty is 4.1 MeV.
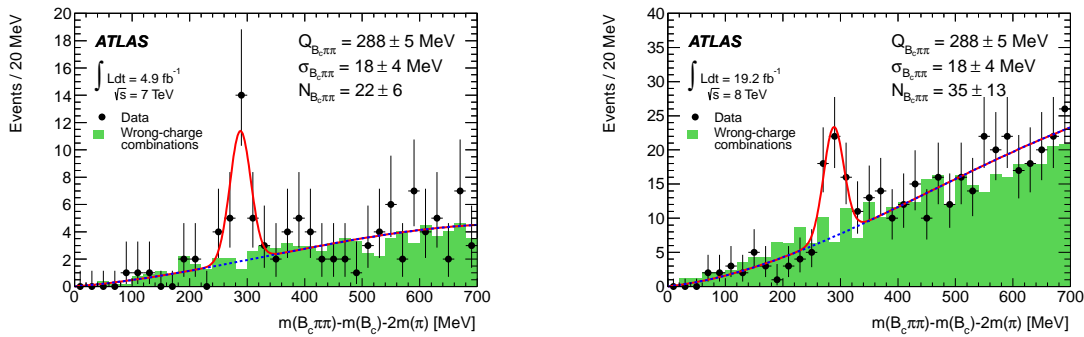

Figure 6. The $m(B_c^\pm \pi\pi) - m(B_c^\pm) - 2m(\pi^\pm)$ distribution in 7 (left) and 8 (right) TeV data.

The significance of the observed structure is evaluated with pseudo-experiments. The mean mass value of the signal contribution is not constrained within the theoretically motivated range to account for a "look elsewhere effect". The significance of the observation is 3.7σ in the 7 TeV data and 4.5σ in the 8 TeV data. The total significance for the combined 7 and 8 TeV dataset is 5.2σ. The error weighted mean mass of the observed structure is $Q = 288.3 \pm 3.5(\text{stat}) \pm 4.1(\text{syst})$ MeV, corresponding to a mass of $6842 \pm 4(\text{stat}) \pm 5(\text{syst})$ MeV. In conclusion, a new state is observed in the ATLAS detector with $4.9\,\text{fb}^{-1}$ of 7 TeV and $19.2\,\text{fb}^{-1}$ of 8 TeV data, consistent with an excited $B_c^\pm(2S)$ state with a predicted mass $m_{B_c(2S)} \sim 6835\text{---}6917$ MeV.

References
[1] ATLAS Collaboration 2014 *Phys. Rev.* D **89** 092009
[2] ATLAS Collaboration 2014 arXiv:1407.1032 [hep-ex], *submitted to Phys. Rev. Lett.*
[3] Cheng H-Y 1997 *Phys. Rev.* D **56** 2799
    Fayyazuddin and Riazuddin 1998 *Phys. Rev.* D **58** 014016
    Mohanta R, Khanna M P, Ishida M, Ishida S and Oda M 1999 *Prog. Theor. Phys.* **101** 959
    Chou C-H, Shih H-H, Lee S-C and Li H-N 2002 *Phys. Rev.* D **65** 074030
    Wei Z-T, Ke H-W and Li X-Q 2009 *Phys. Rev.* D **80** 094016
    Gutsche T, Ivanov M A, Korner J G, Lyubovitskij V E and Santorelli P 2013 *Phys. Rev.* D **88** 114018
[4] Leitner O, Ajaltouni Z and Conte E 2005 *Nucl. Phys.* A **755** 435
    Ajaltouni Z, Conte E and Leitner O 2005 *Phys. Lett.* B **614** 165
[5] ATLAS Collaboration 2008 *JINST* **3** S08003
[6] Beringer J *et al* (Particle Data Group) 2012 *Phys. Rev.* D **86** 010001
[7] Aaij R *et al* (LHCb Collaboration) 2013 *Phys. Lett.* B **724** 27
[8] Godfrey S 2004 *Phys. Rev.* D **70** 054017
    Eichten E and Quigg C 1994 *Phys. Rev.* D **49** 5845
    Kiselev V V, Likhoded A K and Tkabladze A V 1995 *Phys. Rev.* D **51** 3613
    Penin A A, Pineda A, Smirnov V A and Steinhauser M 2004 *Phys. Lett.* B **593** 124
    Dowdall R J, Davis C T H, Hammant T C and Horgan R R 2012 *Phys. Rev.* D **86** 094510